Atmospheric Environment 44 (2010) 4126–4133

Contents lists available at ScienceDirect

Atmospheric Environment

journal homepage: www.elsevier.com/locate/atmosenv

Impact of clouds and aerosols on ozone production in Southeast Texas

James Flynn [a], Barry Lefer [a,*], Bernhard Rappenglück [a], Michael Leuchner [a,1], Ryan Perna [a,2], Jack Dibb [b], Luke Ziemba [b], Casey Anderson [b], Jochen Stutz [c], William Brune [d], Xinrong Ren [d,3], Jingqiu Mao [d,4], Winston Luke [e], Jennifer Olson [f], Gao Chen [f], James Crawford [f]

[a] Department of Earth and Atmospheric Sciences, University of Houston, 4800 Calhoun Rd, Houston, TX 77204-5007, USA
[b] Department of Earth Sciences, University of New Hampshire, 131 Main Street, Durham, NH 03824, USA
[c] Department of Atmospheric and Oceanic Sciences, University of California at Los Angeles, 405 Hilgard Avenue, Los Angeles, CA 90095, USA
[d] Department of Meteorology, Pennsylvania State University, 201 Shields Building, University Park, PA 16802, USA
[e] NOAA Air Resources Laboratory, 1315 East West Highway, Silver Spring, MD 20910, USA
[f] NASA Chemistry and Dynamics Branch, Langley Research Center, Hampton, VA 23681, USA

ARTICLE INFO

Article history:
Received 4 November 2008
Received in revised form
1 September 2009
Accepted 3 September 2009

Keywords:
TexAQS-II
TRAMP
Photolysis rates
Ozone production
Radiative transfer model
Photochemical box model

ABSTRACT

A radiative transfer model and photochemical box model are used to examine the effects of clouds and aerosols on actinic flux and photolysis rates, and the impacts of changes in photolysis rates on ozone production and destruction rates in a polluted urban environment like Houston, Texas. During the TexAQS-II Radical and Aerosol Measurement Project the combined cloud and aerosol effects reduced $j(NO_2)$ photolysis frequencies by nominally 17%, while aerosols reduced $j(NO_2)$ by 3% on six clear sky days. Reductions in actinic flux due to attenuation by clouds and aerosols correspond to reduced net ozone formation rates with a nearly one-to-one relationship. The overall reduction in the net ozone production rate due to reductions in photolysis rates by clouds and aerosols was approximately 8 ppbv h^{-1}.

© 2009 Elsevier Ltd. All rights reserved.

1. Introduction

In 2006, Houston, Texas experienced over 40 days with an 8-h O_3 average over 85 ppbv (TCEQ, 2006 Air Pollution Events). The Houston–Galveston–Brazoria (HGB) eight county area (Brazoria, Chambers, Fort Bend, Galveston, Harris, Liberty, Montgomery, Waller) has been designated as non-attainment by the EPA for violating the ozone standards set forth in the Clean Air Act. Because of the significant ozone problem in the HGB area, efforts to forecast ozone levels are made to help protect sensitive groups and advise the local population when to expect prolonged periods of elevated ozone. The accuracy of these forecast models depends on many factors, including correctly accounting for the radiative effects of clouds and aerosols (Castro et al., 1996; Pour-Biazar et al., 2007).

Tropospheric ozone forms by reactions of oxides of nitrogen (NO_x) and volatile organic compounds (VOCs) in the presence of solar radiation. Ozone photochemistry occurs when NO_2 is photolyzed in sunlight. Ozone formation is the result of the following reactions:

$$NO_2 + h\nu \rightarrow NO + O(^3P) \quad (\text{where } h\nu < 420\ \text{nm}) \tag{1}$$

$$O(^3P) + O_2 + M \rightarrow O_3 + M \tag{2}$$

Once formed, ozone reacts with NO to regenerate NO_2.

$$O_3 + NO \rightarrow NO_2 + O_2 \tag{3}$$

Net ozone production is not possible unless a peroxy radical is present to react with NO to regenerate the NO_2 without destroying an ozone molecule as in reaction (3).

$$RO_2 + NO \rightarrow NO_2 + RO \ (\text{where } R \text{ can be: } H, CH_3, C_2H_5, \text{etc.}) \tag{4}$$

In recent years there has been extensive research into the role of VOCs and NO_x in ozone production in the HGB area. This research

* Corresponding author. Tel.: +1 713 743 3250; fax: +1 713 748 7906.
E-mail address: blefer@uh.edu (B. Lefer).
[1] Now at Fachbereich für Ökoklimatologie, Technische Universität München, Freising, Germany.
[2] Now at Source Environmental, Houston, TX 77027, USA.
[3] Now at Rosenstiel School of Marine and Atmospheric Science, University of Miami, 4600 Rickenbacker Causeway, Miami, FL 33149, USA.
[4] Now at Department of Atmospheric Sciences, Harvard University, 29 Oxford Street, Cambridge, MA 02138, USA.

1352-2310/$ – see front matter © 2009 Elsevier Ltd. All rights reserved.
doi:10.1016/j.atmosenv.2009.09.005

highlights that the local petrochemical emissions, particularly highly reactive VOCs, from the heavily industrialized ship channel area can lead to rapid ozone formation under certain conditions (Ryerson et al., 2003). Research also illustrates the importance of local meteorology and circulation on ozone production (Banta et al., 2005). Lefer et al. (2003) report that ozone photochemistry can be photon limited and has a direct relationship between changes in UV and net ozone production. Without sufficient UV radiation ozone production will be limited, regardless of local circulation patterns or emission sources.

Clouds and aerosols have complex effects on actinic flux photolysis rates in the troposphere and at the surface. Strongly absorbing aerosols can reduce actinic flux at the surface while strongly scattering aerosols can lead to an increase in actinic flux (Jacobson, 1998; Dickerson et al., 1997). Clouds can also enhance or reduce actinic flux depending on their thickness, droplet size, altitude, coverage, and position in the sky (Liao et al., 1999; Lantz et al., 1996).

Previous studies have found that absorbing aerosols reduce UV actinic flux throughout the troposphere, leading to a reduction in near-surface ozone production (Wendisch et al., 1996; Dickerson et al., 1997; Jacobson, 1998). Studies in Los Angeles, California (Jacobson, 1998), and Mexico City (Castro et al., 2001; Raga et al., 2001) and in Sao Paulo, Brazil (de Miranda et al., 2005) found reductions in surface ozone varying from 5 to 30% due to absorbing aerosols. Model predictions have shown an increase in photolysis frequencies in the troposphere in the eastern US, leading to a 5–60% increase in lower tropospheric ozone levels due to strongly scattering aerosols (Dickerson et al., 1997; He and Carmichael, 1999).

During TRACE-P Tang et al. (2003) found that clouds dominated the impacts on short lived radicals like HO_x. Aerosols tended to have more impact on species with a longer lifetime because much of the aerosols tended to be emitted with the precursors and are transported together, exposing the precursors to the aerosol impacts for a longer duration. A plume from Alaskan forest fires transported over long distances found aerosols causing a reduction in ozone production and destruction rates, 18% and 24%, respectively (Real et al., 2007).

Measurements of actinic flux, meteorological parameters, and numerous chemical and aerosol properties were made concurrently on the University of Houston (UH) main campus during the TexAQS 2006 Radical Measurement Project (TRAMP), a six week intensive campaign in August and September 2006 (see Lefer and Rappenglück, in this issue). TRAMP measurements were made on the roof of the 18-story North Moody Tower dormitory located approximately 4 km south of downtown Houston. This elevated location, roughly 70 m above ground, provides a unique opportunity to make continuous measurements that are not directly impacted by surface emissions, and often falls into the second layer of chemical transport models, providing an opportunity for measurement-model comparisons at a location other than the surface where most sampling sites are located (D. Byun, personal communication, 2008). Because direct surface emissions are not likely to be sampled at this elevation, a different view of NO_x partitioning is observed than would be seen at the surface and is more representative of the regional urban atmosphere rather than of small local point and mobile sources. This measurement location also allows for the upward mixing of secondary species formed from surface emissions, which can impact the formation of ozone. Another aspect of the elevated measurement location is the observation of an earlier impact of the residual layer as it mixes down each morning, compared to the surface, and can be affected at night by intermittent turbulence mixing the residual layer downward.

The overall purpose of the TRAMP campaign was to examine the role of radicals on the complex photochemistry in Houston. The work presented here focuses on assessing the impacts of clouds and aerosols on the radiative processes affecting ozone photochemistry. Specifically, how did clouds and aerosols impact the production of O_3 during the TRAMP 2006 campaign, and how do the interactions of radiation and precursors impact the diurnal profile of O_3 production?

2. Methods

Assessment of the impacts of clouds and aerosols on the photochemical environment at the North Moody Tower involved the use of several tools including the LaRC 0-D box model and the NCAR Tropospheric Ultraviolet and Visible radiative transfer model to analyze data collected during TRAMP. Measurements included standard meteorological parameters, actinic flux, ozone, CO, NO/NO_2 (Lefer et al., in this issue), NO_y, SO_2 (Luke et al., in this issue), HONO, HNO_3 (Stutz et al., in this issue), OH, HO_2 (Mao et al., in this issue), PANs, speciated VOC's, H_2O_2, and HCHO (Leuchner and Rappenglueck, in this issue). Several clear sky days during this period are useful in discriminating aerosol effects from cloud effects.

2.1. Models

2.1.1. NCAR – TUV

The National Center for Atmospheric Research (NCAR) Tropospheric Ultraviolet–Visible version 4.1 (TUV) is a cloud free radiative transfer model (CFM) developed to simulate the actinic flux at a given location and has successfully been used for many years and has been shown to perform well (Lefer et al., 2003; Shetter et al., 2003). The TUV model calculated the cloud and aerosol free photolysis rates used to test the sensitivity of the ozone and radical budgets to cloud and aerosol impacts.

The reduction in measured photolysis rates relative to modeled rates are quantified by taking the ratio of an NCAR Scanning Actinic Flux Spectroradiometer (SAFS) derived photolysis rates to those generated by TUV. This ratio is referred to as the *j*-value impact factor (JIF) (Lefer et al., 2003). A JIF less than one indicates a reduction in photolysis rates, while a JIF greater than one indicates an enhancement in the measured photolysis rate as compared to cloud free conditions. Because of uncertainties and instrument limitations, only data collected at solar zenith angles less than 75° (sun sufficiently above the horizon) were used.

2.1.2. LaRC 0-D photochemical box model

Details on the NASA Langley time-dependent box model can be found in Olson et al. (2006) and Crawford et al. (1999). In general, chemical reactions and kinetics are those recommended by Sander et al. (2006). Non-methane hydrocarbon chemistry is based on the modified condensed scheme in Lurmann et al. (1986). For this study, the model is run with either the instantaneous photostationary state assumption (PSS) or in a time-dependent mode using an assumption of diurnal steady state. When sufficient data are available to fully constrain the model, the two methods give essentially identical results for predicted HO_x. The time-dependent mode is useful when observations of moderately-lived HO_x precursor species are missing that cannot be adequately represented by PSS. A comparison of several model mechanisms, including the LaRC mechanism used here, can be found in Chen et al. (in this issue). In addition to the standard model chemical constraints of measurements of O_3, CO, NO_x, acetone, methanol, ethanol, formic and acetic acids, and non-methane hydrocarbons, the model is also constrained by measurements of, HNO_3, PAN, HCHO, H_2O_2, and HONO.

Based on a comparison of $j(NO_2)$ filter radiometer and spectrometer measurements, Crawford et al. (1999) determined that it

was possible to use a cloud correction factor based on $j(NO_2)$ and apply it to other photolysis frequencies. During the campaign there were occasional problems with the SAFS instrument, so gaps in data were filled with data from a MetCon diode array spectroradiometer and Yankee Environmental Systems UV–Vis shadowband radiometers. Because of the differences in the data and limitations in measured wavelengths from these alternate sources, only $j(NO_2)$ photolysis rates were used in this experiment. To account for surface reflection not measured by the SAFS instrument, $j(NO_2)$ observations were increased by 4% (Barnard et al., 2004). The combined uncertainty of the $j(NO_2)$ measurements are 12–15% (Shetter et al., 2003).

Similar to the approach of Lefer et al. (2003), the LaRC model was initially run using SAFS photolysis rates constrained to measured NO_2, allowing the model to calculate PSS NO concentrations based on measured photolysis rates. The resulting total NO_x was then used to constrain the CFM model runs, allowing the calculated photolysis rates to adjust the partitioning of NO_x.

3. Results

3.1. Model sensitivity

To determine the relative importance of the available constraints on net ozone production rates, we ran the model in the time-dependent diurnal equilibrium mode and unconstrained one parameter at a time using measured $j(NO_2)$ photolysis rates. The results from these model runs were then compared to a model run with all parameters constrained and for a selected day containing measurements for all of the potential constraints. Fig. 1 shows the results of this sensitivity test, indicating that in this case, constraining to H_2O_2 and HNO_3 does not significantly change the prediction of HO_x and therefore the predicted net O_3 production, giving a difference of less than 3% from the fully constrained run for the campaign for both species. Unconstraining HCHO and PAN individually results in significant overpredictions in the net ozone production rates occurs, by up to 50% at times. However, unconstraining HONO results in an underprediction of the net ozone production rate. The formation reaction for HONO in the model is the reaction of OH + NO. There has been speculation of additional sources of HONO in the literature from heterogeneous sources and from reactions of an excited state of the NO_2 molecule (Li et al., 2008). An underprediction of such a potentially important radical source significantly impacts the ozone production rates. Similarly, HCHO and PAN are overpredicted in the model leading to overpredicted ozone production rates. It is, therefore, important to constrain the model to observations for these three species for the purposes outlined in this study.

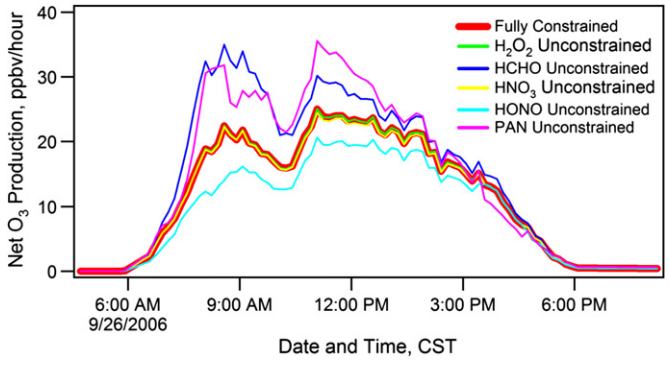

Fig. 1. Net O_3 production rates for September 26, 2006 with fully constrained and unconstrained results.

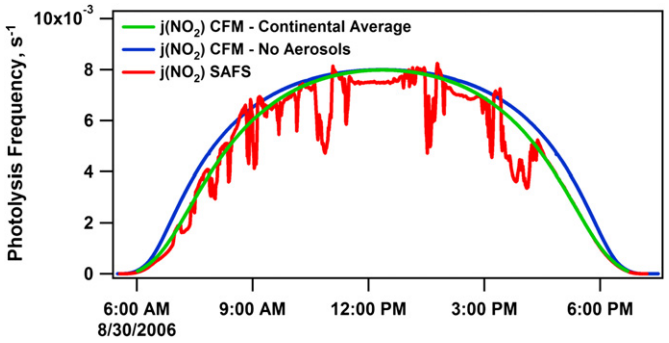

Fig. 2. Diurnal profiles of NO_2 photolysis rates for a partly cloudy day.

3.2. Impact of clouds and aerosols on photolysis rates

Fig. 2 shows the comparison of the $j(NO_2)$ photolysis frequencies calculated from SAFS actinic flux data and the TUV cloud free model using both a continental average aerosol profile and aerosol free conditions. The measured data shows the effects of both clouds and aerosols. The continental average profile compares very well to the measured values in the late afternoon and early evening. The difference between the two cloud free model results shows that effects of aerosols on the $j(NO_2)$ photolysis frequency are more significant in mornings and afternoons than at noon, likely due to the larger airmass factor (path length).

The ratio of the measured photolysis rates to those from TUV without aerosols appears in Fig. 3. Relative to theoretical aerosol free conditions the median JIF for the 47 days of the campaign with available data is 0.83, while for the subset of six cloud free days the median value is 0.97. Fig. 3 shows that for days that include clouds it is possible to have a JIF greater than one indicating that clouds can increase the local actinic flux and thus the photolysis rate. These elevated JIFs are usually short lived and are caused by reflections and other interactions with nearby clouds that do not block the direct beam of the sun but rather increase the diffuse downwelling radiation at the measurement point. These momentary enhancements in photochemistry are often offset to a greater extent by the shadow of the cloud as it often blocks the direct beam component immediately prior to or after the enhancements. These enhancements can be seen in Fig. 2 where the measured SAFS curve is

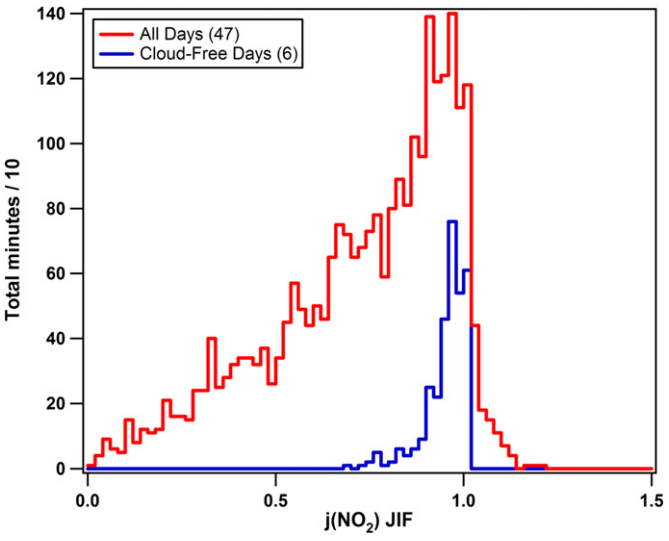

Fig. 3. Histogram of JIF for all days and six cloud free days.

higher than the blue aerosol free curve. Under cloud free conditions all of the JIFs are at a value of close to one or less. This indicates that the aerosols in Houston may have reduced the $j(NO_2)$ by nominally 3% for these six days, while for the overall campaign clouds and aerosols combined to reduce $j(NO_2)$ by nominally 17%.

The changes in the actinic flux by clouds and aerosols impact the photochemical processes that produce ozone. By altering the photolysis rates involved in ozone production and destruction, changes in actinic flux can drastically change the net ozone production rates and the balance of how the various reactions control these rates.

3.3. Impact of clouds and aerosols on ozone production

Taking the campaign average of the ozone formation ($HO_2 + NO$, $CH_3O_2 + NO$, $RO_2 + NO$), chemical loss ($O^1D + H_2O$, $HO_2 + O_3$, $O_3 + OH$, $NO_2 + OH$, $O_3 + NMHC$), and net ozone production terms (formation minus loss) calculated within the LaRC model for both CFM and SAFS photolysis rates provides the data for Fig. 4. The difference between the average ozone destruction terms for the two photolysis rates is minimal, while the figure reveals a much more significant difference between the two ozone formation, and thus the net production, rates. On average, clouds and aerosols reduced the net ozone production rate from 23.1 to 14.9 ppbv h^{-1}. Because average values may mask interesting details, two days will be examined in more detail in the following section.

To quantify the effects of changes in the JIF on ozone production and loss rates, Fig. 5 plots the ratio of the ozone production and loss terms from the SAFS to the CFM modeled photolysis rates versus the JIF. Median values for the modeled daytime periods for O_3 formation and destruction are approximately 15 and 1 ppbv h^{-1}, respectively. As shown in Fig. 5, both of the ozone loss and production terms are nearly linear and fall close to the 1:1 line. This indicates that a 50% reduction in actinic flux compared to clear sky values (JIF of 0.5) results in roughly a 60% reduction in ozone production and a 40% reduction in ozone loss rates. While all production terms are photolytically driven, not all of the destruction terms are. The $O_3 + NMHC$ term has no significant dependence on radiation, reducing the relative impact of lower radiation on the collective O_3 destruction rate.

When breaking down the actual production and loss terms for measured and calculated photolysis rates into a median diurnal profile for days with greater than 11 h of data (Fig. 6a and b), we see that ozone production rates peak midday in the 1100–1200 CST

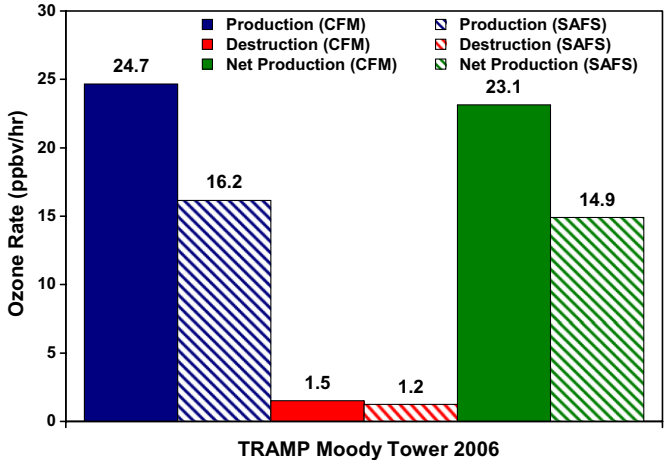

Fig. 4. Campaign average ozone production and loss terms.

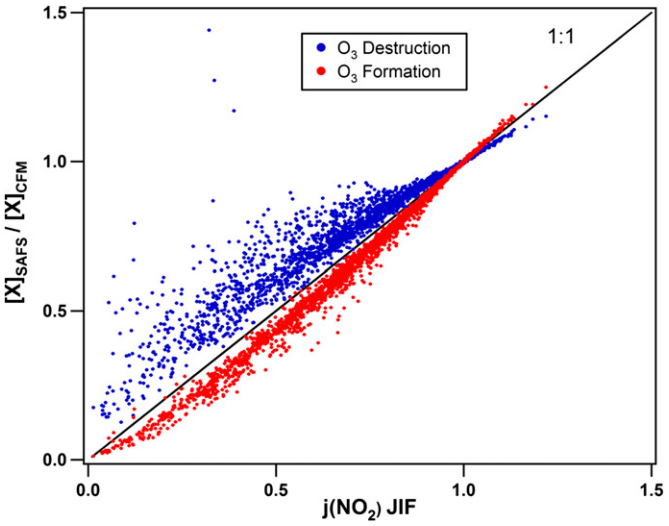

Fig. 5. Ratio of ozone formation and loss terms using SAFS and TUV photolysis rates against $j(NO_2)$ JIF.

hour at just over 25 ppbv h^{-1} using SAFS photolysis rates. For the same data using the CFM simulated cloud and aerosol free photolysis rates, the instantaneous ozone production rate increases to greater than 35 ppbv h^{-1} and shifts an hour earlier. Fig. 6b shows the loss rates for both photolysis rates. This plot shows that the loss

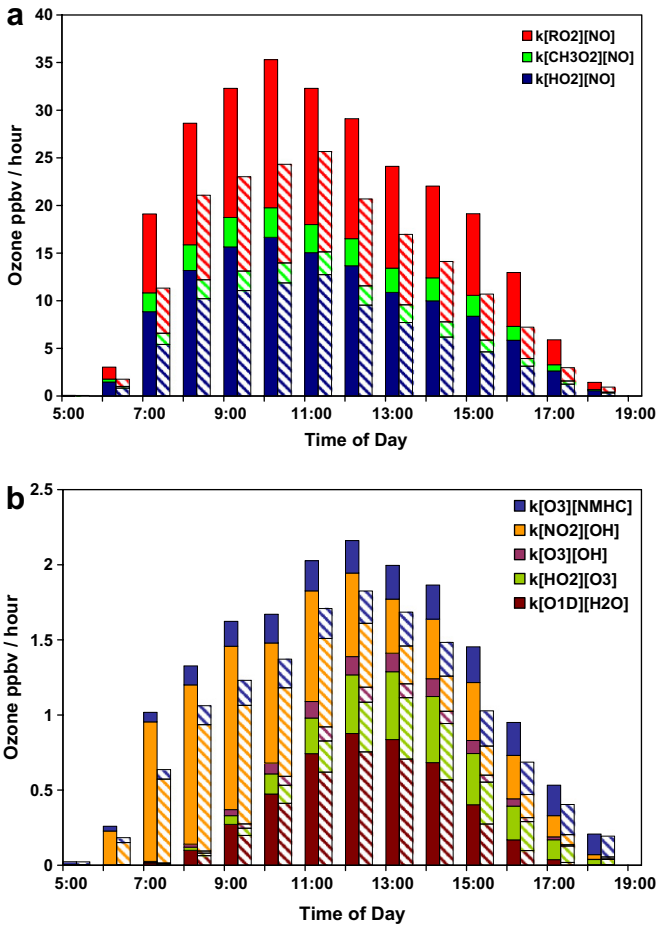

Fig. 6. Diurnal profile of median instantaneous ozone formation (a) and loss (b) rates for the entire campaign. Solid and striped bars are for CFM and SAFS, respectively.

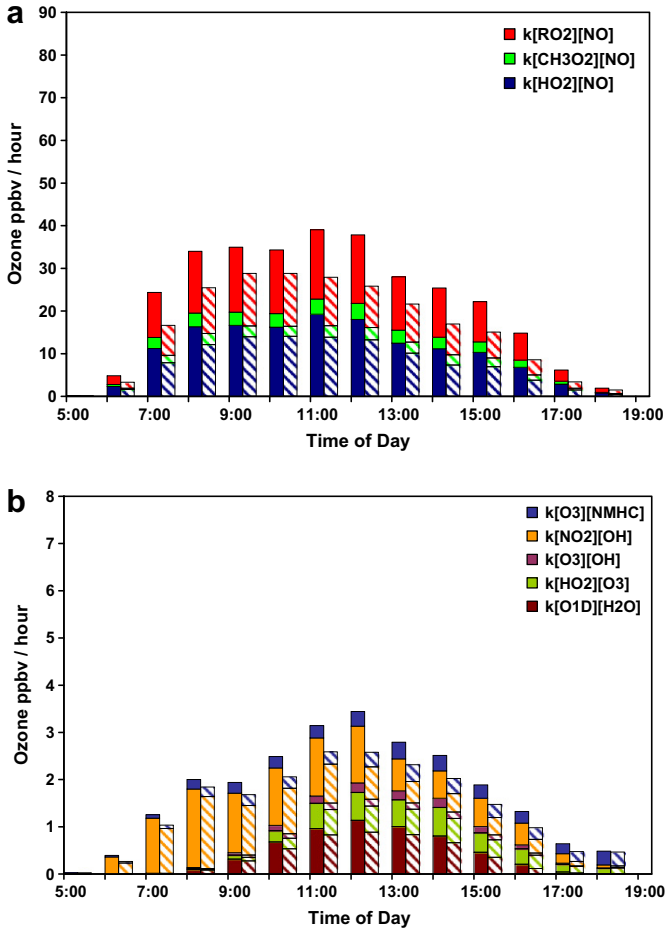

Fig. 7. Diurnal profile of median instantaneous ozone formation (a) and loss (b) rates for 10 intensive radiosonde launch days. Solid and striped bars are for CFM and SAFS, respectively.

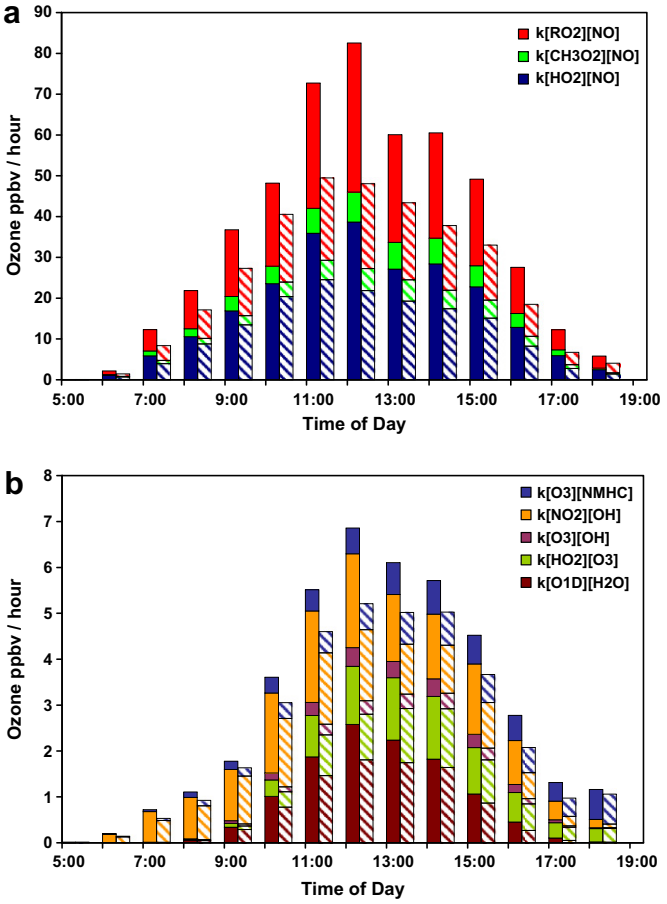

Fig. 8. Diurnal profile of median instantaneous ozone formation (a) and loss (b) rates for 10 intensive radiosonde launch days normalized to boundary layer height. Solid and striped bars are for CFM and SAFS, respectively.

rates are quite small throughout the entire daytime period compared to the production rates.

Fig. 7a and b show the median diurnal profile of ozone formation and destruction rates for ten days with intensive radiosonde launches. These intensive days were forecast to have high ozone and typically included at least six launches per day spaced 3 h apart from early morning through late evening, and continued throughout the night in some cases. Peak ozone production with measured photolysis rates peak in the 0900–1100 CST hours at almost 30 ppbv h^{-1}, while the cloud and aerosol free photolysis rates move the peak production later to the 1100–1200 CST period with a production rate approaching 40 ppbv h^{-1}.

We then adjusted this data to account for boundary layer heights to see how boundary layer height may impact total boundary layer ozone production in Houston. For each of the ten intensive radiosonde days selected, the boundary layer heights were interpolated to 10-min resolution. Then we calculated a correction factor by taking the ratio of the interpolated measured boundary layer heights to the campaign median measured height of 700 m as a proxy representative of an integrated O_3 production amount. Multiplying the ozone formation and destruction rates by this ratio allowed for normalization of the rates to a boundary layer height of 700 m. Fig. 8a and b show the results of this adjustment. Using normalized data shifts the peak production more towards the middle of the day for both measured and modeled photolysis rates.

4. Discussion

As part of a more detailed inspection of the data, we selected two days to further examine ozone production rates and factors that impact these rates. Several factors impact ozone production rates, including the amount of ozone precursors present and the availability of sunlight. High levels of ozone precursors can result from the proximity to the emission sources, shallow boundary layer depths, a lack of dilution by high wind speeds, or any combination of these factors. As previously shown, clouds can limit the amount of radiation reaching the surface, controlling the photochemical production of ozone. In addition to regulating the rate of ozone production, the reduction in solar radiation reaching the surface can also suppress boundary layer growth, thus impacting concentrations of ozone precursors.

4.1. August 31–September 1, 2006 – Clear skies with low morning boundary layer

Some of the largest ozone production rates from the LaRC model using both SAFS and TUV photolysis rates occurred on August 31, 2006 with calculated net production approaching 352 ppbv day^{-1} using SAFS $j(NO_2)$ and 416 ppbv day^{-1} using TUV derived $j(NO_2)$ photolysis rates. The total ozone produced per day was calculated by summing ozone produced per model step as determined from the ozone production rates.

The 31st was cloud free with no rain. Winds on this day rotated clockwise from north to south over the course of the day, which is

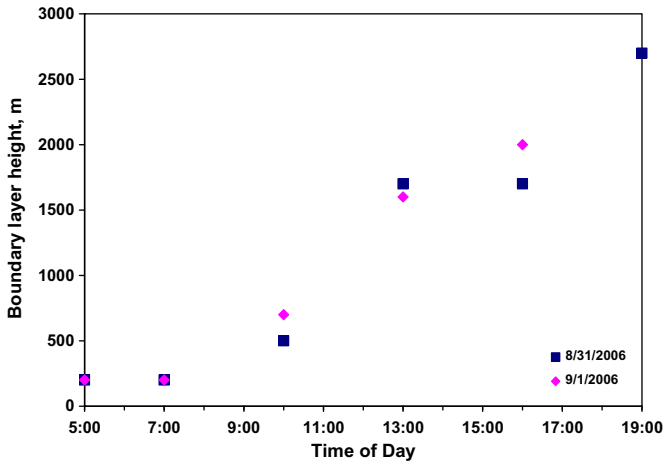

Fig. 9. Boundary layer heights for August 31 and September 1, 2006.

typical for the Coriolis driven forcing of the local sea-breeze system at this latitude under weak synoptic conditions (Banta et al., 2005), with daytime winds predominately from the northeast to east and with speeds under 2 m s^{-1} for the majority of the daytime period. Temperatures on this day were around 35 °C. September 1 was partly cloudy from mid-morning through the evening and saw similar temperatures as the previous day, with slightly higher relative humidity. Wind speeds again were relatively light throughout most of the daytime period, increasing in speed as sunset approached, while the wind direction continued the clockwise rotation from the previous day through north before becoming variable through the afternoon. A more detailed discussion of the boundary layer structure and the land sea-breeze variations on these two days can be found in Rappenglück et al. (2008). The nighttime boundary layer during the night August 31–September 1 including the morning transition period on September 01 is described in Day et al. (in this issue).

August 31 shows an interesting case where the diurnal ozone formation and destruction rates are negatively correlated with boundary layer height. Fig. 9 shows low morning boundary layer heights from 0400 to 0900 CST (between less than 200 up to 500 m), resulting in increased NO_x and VOC levels which correlate with the very high average ozone production rates calculated in the LaRC model seen in Fig. 10a. Using measured photolysis rates these rates peak between 0900 and 1000 CST in excess of 114 ppbv h^{-1} and almost 141 ppbv h^{-1} with clear sky photolysis rates. Measured ozone values on the 31st increased rapidly from 6 ppbv at 7:05 am CST to 106 ppbv by 9:35 am, ultimately reaching a peak 10-min value of 136 ppbv at 5:05 pm. Boundary layer heights on the following day were very similar through noon; however, the NO_x and VOC measurements were much lower, resulting in lower ozone formation and destruction rates. Measured ozone levels during the night of the 31st–1st show relatively constant values around 60 ppbv. These elevated levels, coupled with the daytime ozone formation and destruction rates, resulted in roughly the same peak ozone levels even though the formation and destruction rates were much lower than those from the previous day (Fig. 11a and b).

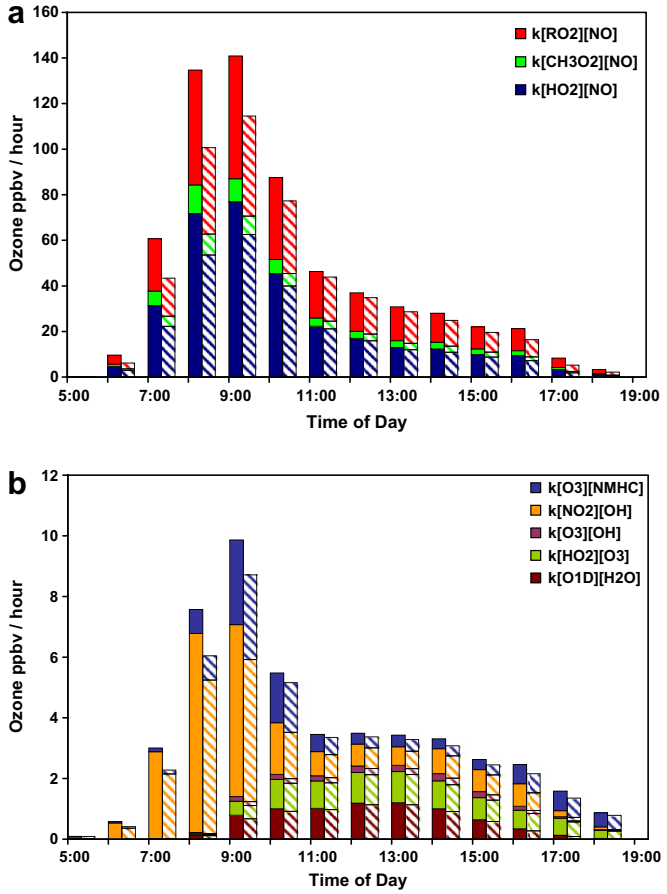

Fig. 10. August 31, 2006 diurnal ozone formation (a) and loss (b) profile. Solid and striped bars are for CFM and SAFS, respectively.

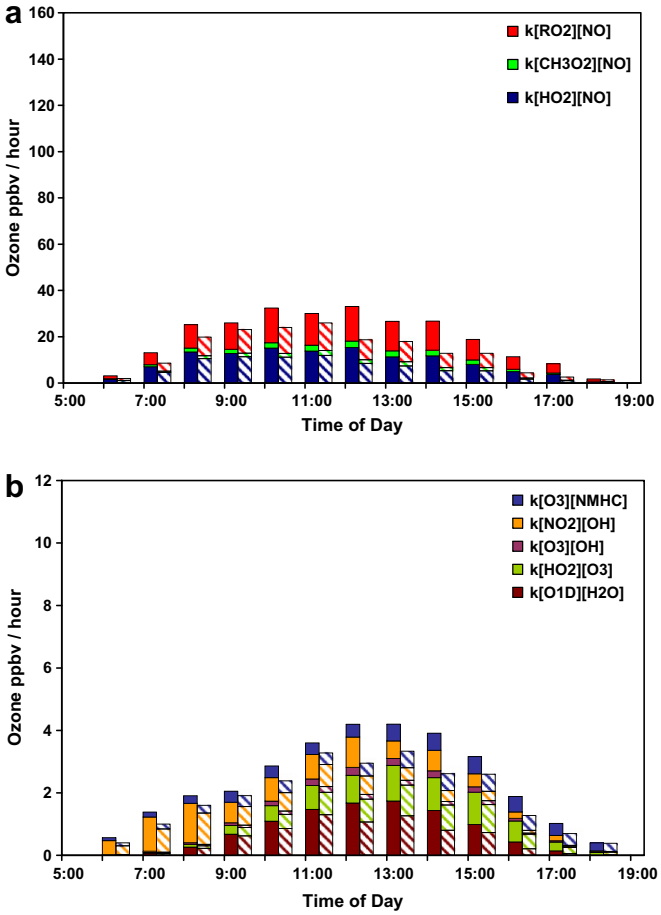

Fig. 11. September 1, 2006 diurnal ozone formation (a) and loss (b) profile. Solid and striped bars are for CFM and SAFS, respectively.

In line with assumptions stated in Rappenglück et al. (2008) industrial emissions were most likely be transported to the Moody Tower during the early morning hours of the 31st by the north-easterly flows typical for the onset of Galveston bay breeze. These emissions coupled with the low boundary layer height resulted in the high NO_x and VOC levels observed at the Moody Tower. The morning's clear skies and high ozone precursor levels combined to cause the rapid ozone formation rates. As the day progressed boundary layer heights grew, diluting the ozone precursor levels, resulting in decreased ozone production rates for the remainder of the day. In contrast, winds on September 1st show that the flow approached the Moody Tower from the northwest, a sector with relatively low emissions. With the morning of September 1st being clear with similar boundary layer heights, ozone production rates were much lower because of lower levels of ozone precursors.

From this example, we see that ozone production rates in Houston can peak in the morning, responding to the effects of large quantities of ozone precursors being emitted into a shallow boundary layer, and that wind direction plays a critical role on the ozone production rates at the Moody Tower.

5. Conclusions and future work

A significant number of ozone events that exceed the regulatory standards occur in the Houston-Galveston-Brazoria area every year and these events may adversely affect the health of the local population. In order to improve the ability of ozone models to accurately predict episodes that may lead to unhealthy conditions, it will be necessary to better quantify the effects of clouds and aerosols. During the campaign, combined cloud and aerosol effects dominated reductions in photolysis frequencies compared to aerosols only effects by 17 and 3% respectively. Reductions in actinic flux due to attenuation by clouds and aerosols correspond to reduced net ozone formation rates with a nearly one-to-one relationship. The overall reduction in the net ozone production rate due to reductions in photolysis rates by clouds and aerosols was approximately 8 ppbv h^{-1}.

For the Houston area, HONO, HCHO, and PAN are important measurements that are needed as constraints for accurate predictions of HO_x and O_3 production. Ozone destruction rates are quite small in comparison to the formation rates and only contribute to a loss of a few ppbv h^{-1}. The median diurnal profile of ozone production rates peaks in the 1100–1200 CST hour at just over 25 ppbv h^{-1} using measured photolysis rates. For the same time using the simulated cloud and aerosol free photolysis rates, the instantaneous ozone production rate increases to greater than 35 ppbv h^{-1} and shifts an hour earlier. The late morning peak with the CFM photolysis rates may be due to having enough incoming solar radiation while the boundary layer is relatively low, leading to an accumulation of ozone precursors from morning rush hour and continuous industrial emissions. When scaled to a constant boundary layer height, this morning peak in ozone production shifts to the midday period.

Future work will entail a more extensive evaluation of the results when using HONO and HCHO determined from long-path DOAS measurements. Particular attention will be paid to those times with significant discrepancies between the in situ HONO and DOAS data (Stutz et al., in this issue). Additionally, a comparison of these results with those from a newly released version of the LaRC model which includes NO_2^* reactions (Li et al., 2008) will be performed to examine if the changes in modeled HO_x and HONO are significant.

Acknowledgements

We would like to thank the Houston Advanced Research Center and the Texas Commission on Environmental Quality for their financial support. We would also like to thank the USDA-UVB monitoring program, Fong Ngan, Daewon Byun, and Mark Estes for providing assistance in data analysis and guidance.

References

Banta, R.M., Senff, C.J., Nielsen-Gammon, J., Darby, L.S., Ryerson, T.B., Alvarez, R.J., Sandberg, S.P., Williams, E.J., Trainer, M., 2005. A bad air day in Houston. Bull. Am. Meteorol. Soc. 86, 657–669.

Barnard, J.C., Chapman, E.G., Fast, J.D., Schmelzer, J.R., Slusser, J.R., Shetter, R.E., 2004. An evaluation of the FAST-J photolysis algorithm for predicting nitrogen dioxide photolysis rates under clear and cloudy sjy conditions. Atmos. Environ. 38 (21), 3393–3403.

Castro, T., et al., 1996. Sensitivity analysis of a uv radiation transfer model and experimental photolysis rates of NO_2 in the atmosphere of Mexico City. Atmos. Environ. 31 (4), 609–620.

Castro, T., et al., 2001. The influence of aerosols on photochemical smog in Mexico City. Atmos. Environ. 35, 1765–1772.

Chen, S., Ren, X., Mao, J., Chen, Z., Brune, W., Lefer, B., Rappenglück, B., Flynn, J., Olson, J., Crawford, J.H. A comparison of chemical mechanisms based on TRAMP-2006 field data, in this issue.

Crawford, J., et al., 1999. An assessment of cloud effects on photolysis rate coefficients: comparison of experimental and theoretical values. J. Geophys. Res. 104 (D5), 5725–5734.

Day, B.M., Rappenglück, B., Clements, C.B., Tucker, S.C., Brewer, W.A. Characteristics of the nocturnal boundary layer in Houston, Texas during TexAQS II, in this issue.

de Miranda, R., Andrade, M.F., Fattori, A.P., 2005. Preliminary studies of the effect of aerosols on nitrogen dioxide photolysis rates in the city of Sao Paulo, Brazil. Atmos. Environ. 75, 135–148.

Dickerson, R.R., Kondragunta, S., Stenchikov, G., Civerolo, K.L., Doddridge, B.G., Holben, N., 1997. The impact of aerosols on solar ultraviolet radiation and photochemical smog. Science 278, 827–830.

He, S., Carmichael, G.R., 1999. Sensitivity of photolysis rates and ozone production in the troposphere to aerosol properties. J. Geophys. Res. 104 (D21), 26307–26324.

Jacobson, M.Z., 1998. Studying the effects of aerosols on vertical photolysis rate coefficient and temperature profiles over an urban airshed. J. Geophys. Res. 103 (D9), 10593–10604.

Lantz, K.O., Shetter, R.E., Cantrell, C.A., Flocke, S.J., Calvert, J.G., Madronich, S., 1996. Theoretical, actinometric, and radiometric determinations of the photolysis rate coefficient of NO_2 during the Mauna Loa observatory photochemistry experiment 2. J. Geophys. Res. 101 (D9), 14613–14629.

Lefer, B.L., Shetter, R.E., Hall, S.R., Crawford, J.H., Olson, J.R., 2003. Impact of clouds and aerosols on photolysis frequencies and photochemistry during TRACE-P: 1. Analysis using radiative transfer and photochemical box models. J. Geophys. Res. 108 (D21), 8821. doi:10.1029/2002JD003171.

Lefer, B., Rappenglück, B., Flynn, J., Haman, C. Photochemical and meteorological climate during the Texas-II Radical and Aerosol Measurement Project (TRAMP), in this issue.

Lefer, B., Rappenglück, B. TRAMP overview, in this issue.

Leuchner, M., Rappenglueck, B. VOC source–receptor relationships in Houston during TEXAQS-II, in this issue.

Li, S., Matthews, J., Sinha, A., 2008. Atmospheric hydroxyl radical production from electronically excited NO_2 and H_2O. Science 5870, 1657–1660. doi:10.1126/science.1151443.

Liao, H., Yung, Y., Seinfeld, J., 1999. Effects of aerosols on tropospheric photolysis rates in clear and cloudy atmospheres. J. Geophys. Res. 104 (D19), 23697–23707.

Luke, W., Kelley, P., Lefer, B., Flynn, J., Rappenglück, B., Leuchner, M., Dibb, J., Ziemba, L., Anderson, C., Buhr, M. Measurements of primary trace gases and NO_y composition during TRAMP, in this issue.

Lurmann, F.W., Lloyd, A.C., Atkinson, R., 1986. A chemical mechanism for use in long-range transport/acid deposition computer modeling. J. Geophys. Res. 91, 10905–10936.

Mao, J., Ren, X., Chen, S., Brune, W., Chen, Z., Martinez, M., Harder, H., Lefer, B., Rappenglück, B., Flynn, J., Leuchner, M. Atmospheric oxidation capacity in the summer of Houston 2006: comparison with summer measurements in other metropolitan studies, in this issue.

Olson, J.R., Crawford, J.H., Chen, G., Brune, W.H., Faloona, I.C., Tan, D., Harder, H., Martinez, M., 2006. A reevaluation of airborne HO_x observations from NASA field campaigns. J. Geophys. Res. 111, D10301. doi:10.1029/2005JD006617.

Pour-Biazar, A., et al., 2007. Correcting photolysis rates on the basis of satellite observed clouds. J. Geophys. Res. 112, D10302. doi:10.1029/2006JD007422.

Raga, G.B., Castro, T., Baumgardner, D., 2001. The impact of megacity pollution on local climate and implications for the regional environment: Mexico City. Atmos. Environ. 35, 1805–1811.

Rappenglück, B., Perna, R., Zhong, S., Morris, G.A., 2008. An analysis of the vertical structure of the atmosphere and the upper-level meteorology and their impact on surface ozone levels in Houston, Texas. J. Geophys. Res. 113, D17315. doi:10.1029/2007JD009745.

Real, E., et al., 2007. Processes influencing ozone levels in Alaskan forest fire plumes during long-range transport over the North Atlantic. J. Geophys. Res. 112, D10S41. doi:10.1029/2006JD007576.

Ryerson, T.B., et al., 2003. Effect of petrochemical industrial emissions of reactive alkenes and NO_x on tropospheric ozone formation in Houston, Texas. J. Geophys. Res. 108 (D8), 4249. doi:10.1029/2002JD003070.

Sander, S., Friedl, R.R., Ravishankara, A.R., Golden, D.M., Kolb, C.E., Kurylo, M.J., Molina, M.J., Moortgat, G.K., Keller-Rudek, H., Finlayson-Pitts, B.J., Wine, P.H., Huie, R.E., Orkin, V.L. Chemical Kinetics and Photochemical Data for Use in Atmospheric Studies. Evaluation Number 15, JPL Publication 06–2, 2006.

Shetter, R.E., et al., 2003. Photolysis frequency of NO_2: measurement and modeling during the International Photolysis Frequency Measurement and Modeling Intercomparison (IPMMI). J. Geophys. Res. 108 (D16), 8544. doi:10.1029/2002JD002932.

Stutz, J., Oh, H., Whitlow, S., Anderson, C., Dibb, J., Flynn, J., Rappenglück, B., Lefer, B. Intercomparison of DOAS and Mist-chamber IC measurements of HONO in Houston, TX, in this issue.

Tang, Y., et al., 2003. Impacts of aerosols and clouds on photolysis frequencies and photochemistry during TRACE-P: 2. Three-dimensional study using a regional chemical transport model. J. Geophys. Res. 108 (D21), 8822. doi:10.1029/2002JD003100.

Texas Commission for Environmental Quality, 2006. Air Pollution Events, http://www.tceq.state.tx.us/compliance/monitoring/air/monops/sigevents06.html.

Wendisch, M., Mertes, S., Ruggaber, A., Nakajima, T., 1996. Vertical profiles of aerosol and radiation and the influence of a temperature inversion: measurements and radiative transfer calculations. J. Appl. Meteorol. 35 (10), 1703–1715.